

A Unified Motion-Based Framework for Mass, Energy, and Toroidal Solitons: A Continuum Theory of Stationary Organized Motion

Ivan Salines
Independent Researcher

November 12, 2025

Abstract

We propose a physical framework in which mass, energy, and particle-like structures arise from organized patterns of motion in a continuous medium. The fundamental fields of the theory are the density of motion $\rho(x)$ and a phase of motion $\theta(x)$, with a velocity field emerging from the gradient of the phase. Energy is interpreted as “quantity of motion squared”, while mass appears as a stationary configuration of internal motion. Within this framework we identify a class of self-organized, localized, toroidal solutions whose geometry is quantized by a winding number. We derive the reduced toroidal equations, the effective potential, an existence condition for soliton-like profiles, and a variational estimate of the equilibrium radius. We show that the transverse soliton equation belongs to the same mathematical class as Q-ball equations, and we present a numerical exploration demonstrating that the theory lies within a well-known soliton-supporting regime. We further analyze the effective well structure, introduce a tuned family of potentials, and perform a refined parameter scan that reveals quasi-localized profiles lying at the edge of the solitonic window. Finally, Appendix D provides a linear stability analysis of the toroidal soliton equation.

Contents

1	Introduction	2
2	Related Work and Novelty	2
3	Motion Fields and Energy Functional	3
4	Toroidal Configurations of Organized Motion	3
5	Variational Estimate of the Equilibrium Radius	4
6	Discussion and Outlook	4

1 Introduction

The objective of this work is to explore a minimal and conceptually transparent physical framework in which mass and energy emerge from organized motion in a continuous medium. In this perspective:

Energy is motion, and mass is stationary organized motion.

We take as fundamental fields the density of motion $\rho(x)$ and a phase of motion $\theta(x)$. The velocity is derived from the phase gradient, and the dynamical content comes from a Lagrangian of the form $\mathcal{L} = \rho v^2 - U(\rho)$.

A central idea of this work is that localized particle-like structures correspond to stable, self-organized patterns of motion. A natural configuration of this type is a toroidal arrangement of circulating motion, parametrized by a winding number. Such ring-like structures appear in fluid vortex dynamics, Q-ball solitons, vorton solutions, and knotted field configurations. Here we show that toroidal solitons emerge naturally in the present motion-based continuum theory.

We derive the effective equation governing the transverse profile of the toroidal configuration, exhibit its connection to Q-ball radial equations, compute equilibrium conditions, and investigate numerical evidence for solitonic behaviour. We then refine the analysis of the effective potential well and perform a tuned and subsequently refined scan in parameter space, demonstrating that the model indeed lies in a Q-ball-like regime near the solitonic window. Appendix D contains the linear stability analysis of the transverse equation.

2 Related Work and Novelty

The present framework is conceptually related to several established lines of research:

- **Non-topological solitons and Q-balls**, where a complex scalar field with a suitable self-interaction supports localized lumps of finite charge;
- **Toroidal and ring-like solitons**, including Q-rings, vortons, and knotted configurations in various field theories;
- **Vortex rings and toroidal structures** in hydrodynamics and superfluid systems, where circulation is quantized by an integer winding number.

Traditional approaches typically start from a complex scalar field Φ and derive radial equations for a modulus $f(r)$ and a global phase rotation $e^{i\Omega t}$, possibly with additional spatial winding. In contrast, the present work starts from a *motion-based* decomposition in which the fundamental variables are the density of motion ρ and the phase of motion θ , and the Lagrangian is interpreted as “density times velocity squared minus a potential of density”.

This shift of emphasis leads to several novel features:

- Toroidal configurations arise naturally as self-organized patterns of motion, with the winding number n quantizing the geometry rather than being introduced as an external topological constraint.
- The reduced transverse equation is explicitly connected to Q-ball–type radial equations, allowing us to import existence criteria and stability insights from that literature.
- The refined numerical scan in the parameter space of the effective potential reveals a narrow “pre-solitonic” window in which quasi-localized profiles exist, clarifying the proximity of the model to genuine soliton-supporting regimes.

In this sense, the present work can be seen as a bridge between Q-ball–like non-topological solitons, toroidal/vorton configurations, and a broader continuum interpretation in which mass and energy are manifestations of organized motion.

3 Motion Fields and Energy Functional

We work with two fields:

- the *density of motion* $\rho(x)$,
- the *phase of motion* $\theta(x)$.

The velocity field is

$$v_\mu = \partial_\mu \theta.$$

The Lagrangian density is

$$\mathcal{L} = \rho v^\mu v_\mu - U(\rho),$$

and the corresponding energy functional is

$$E = \int (\rho v^2 + U(\rho)) d^3x.$$

A configuration contributes to *mass* when the motion is internal and stationary in space but carries internal oscillation. Thus mass appears as stationary organized motion, whereas energy is the square of the quantity of motion.

4 Toroidal Configurations of Organized Motion

We consider a toroidal geometry with major radius R and transverse coordinates (σ, χ) on the cross-section. We adopt the phase ansatz

$$\theta(t, \sigma, \chi) = \Omega t + n\chi,$$

with integer winding $n \in \mathbb{Z}$.

The corresponding velocity field is

$$v^2 = (\partial_t \theta)^2 + \frac{1}{\sigma^2} (\partial_\chi \theta)^2 = \Omega^2 + \frac{n^2}{\sigma^2}.$$

In the thin-torus approximation, the energy reduces to

$$E[\rho] = 2\pi \int_0^\infty \left[\rho(\Omega^2 + \frac{n^2}{R^2}) + (\nabla \rho)^2 + U(\rho) \right] \sigma d\sigma.$$

Toroidal configurations are thus encoded in the radial profile $\rho(\sigma)$ and in the parameters (Ω, n, R) , with n providing a natural winding quantization condition.

5 Variational Estimate of the Equilibrium Radius

The dependence of the total energy on the major radius R may be schematically cast in the form

$$E(R) = AR^2 + \frac{B}{R^2} + C,$$

where A collects contributions that grow with the size of the torus, B those that shrink with R , and C is the internal energy of the profile.

Minimizing with respect to R yields

$$R_* = (B/A)^{1/4}, \quad E_* = 2\sqrt{AB} + C.$$

This implies a geometrical quantization of the equilibrium radius $R_* \sim |n|$ once the dependence of A and B on n is taken into account, and provides a first link between winding number and effective mass of the configuration.

6 Discussion and Outlook

The analysis developed in this work shows that a simple motion-based continuum theory can sustain toroidal, self-organized configurations whose transverse dynamics is governed by a Q-ball-type equation. The toroidal ansatz with phase

$$\theta(t, \sigma, \chi) = \Omega t + n\chi$$

naturally implements quantized circulation through the integer winding number n , while the density field $\rho(\sigma)$ encodes how the medium of motion self-organizes in the cross-section of the torus.

The effective potential $U_{\text{eff}}(\rho)$, constructed from a sextic density potential and the kinetic contribution of the phase, exhibits the characteristic structure required for non-topological solitons: a nontrivial minimum at finite $\rho_0 > 0$ and a well deep enough to support bound configurations. The refined analysis of the function $f(\rho) = U(\rho)/\rho^2$ confirms that the present model lies in the same mathematical class as Q-ball-supporting theories.

At the level of the reduced transverse equation, the numerical explorations show that:

- the system admits regular profiles for a broad range of central amplitudes ρ_c and frequencies Ω ;
- a tuned family of potentials with parameters (ε, λ) deepens and broadens the effective well, moving the system closer to a true soliton-supporting regime;
- an ultra-refined scan in (Ω, ρ_c) reveals quasi-localized profiles with small-amplitude, low-curvature oscillatory tails, which we interpret as “pre-solitonic” solutions at the edge of the existence window.

Physically, these results support the picture in which a toroidal soliton represents a localized, stationary pattern of organized motion, with mass corresponding to the amount of motion bound in the structure and the winding number n fixing its geometry. The reduced 2D problem captures the essential competition between gradient energy and potential energy, while the full 3D construction wraps this transverse solution on a circle of radius R , leading to a self-consistent ring-like configuration.

Future work should extend the present analysis in at least three directions:

1. Construction of fully localized 3D toroidal configurations using the insights obtained from the 2D radial reduction;
2. Numerical evaluation of the spectrum of the linear operator governing small perturbations around the transverse profile, following the Sturm–Liouville structure outlined in Appendix D;
3. Coupling of the motion-based framework to additional fields or external potentials, to explore possible analogues in condensed matter, superfluid systems, or effective field theories of matter.

In all cases, the underlying interpretation remains the same: mass and structured energy distributions emerge as stationary, self-organized patterns of motion in a continuous medium.

7 Predictions and Limitations

Predictions

Within the present framework and its toroidal reduction, several qualitative and semi-quantitative predictions can be formulated:

- **Geometric quantization of the radius.** The variational estimate $E(R) = AR^2 + B/R^2 + C$ implies a preferred radius $R_* \propto (B/A)^{1/4}$, which, once the dependence of A and B on the winding n is included, suggests $R_* \sim |n|^{1/2}$ or a similar scaling, i.e. a geometric quantization of the torus size.
- **Narrow solitonic window.** The refined scan in (Ω, ρ_c) reveals that quasi-localized profiles occur only in a narrow band of parameters with $\Omega \lesssim 1$ and moderate ρ_c , a typical feature of Q-ball–like systems near the existence threshold.

- **Pre-solitonic tails.** The best configurations in the tuned potential exhibit tails with small amplitude and low curvature, indicating that a full 3D toroidal construction in the same parameter region should admit genuinely localized solitons.
- **Stability channels.** The structure of the linearized operator in Appendix D suggests a discrete spectrum of small oscillation modes (breathing, modulation, surface modes), with stability tied to the absence of negative eigenvalues.

Limitations

At the same time, the present analysis is subject to several important limitations:

- **Reduced dimensionality.** The transverse equation is a 2D radial reduction of a 3D toroidal problem. While it captures key features of the core and tail, full localization and stability must ultimately be assessed in the complete 3D geometry.
- **Classical mean-field description.** The framework is classical and does not include quantum corrections or fluctuations of the motion field, which may be relevant for small-scale or high-energy configurations.
- **Phenomenological potential.** The sextic potential and its tuned variants are chosen for their mathematical and structural properties. A microphysical derivation of $U(\rho)$ from an underlying field theory or condensed-matter analogue remains an open problem.
- **Partial stability analysis.** Appendix D outlines the linear stability operator but does not compute the eigenvalue spectrum. A full numerical diagonalization is required to definitively classify stable versus unstable configurations.

Despite these limitations, the present work demonstrates that a simple, motion-based continuum model is structurally capable of supporting toroidal soliton-like configurations and provides a concrete roadmap for their further analytical and numerical investigation.

Appendix A — Variation and Equations of Motion

Variation with respect to θ yields the continuity-like equation

$$\partial_\mu(\rho \partial^\mu \theta) = 0.$$

Variation with respect to ρ yields the local relation

$$v^2 = U'(\rho),$$

which connects the velocity of the motion field to the slope of the potential. This provides a closure condition for the model once $U(\rho)$ is specified.

Appendix B — Effective Potential Construction

We adopt a sextic potential of the form

$$U(\rho) = \frac{1}{2}m^2\rho^2 - \frac{1}{4}g\rho^4 + \frac{\lambda}{6}\rho^6, \quad m^2 > 0, g > 0, \lambda > 0,$$

which is widely used in Q-ball and non-topological soliton studies.

In the presence of a time-dependent phase rotation with frequency Ω and toroidal winding n , the effective potential can be defined as

$$U_{\text{eff}}(\rho) = U(\rho) + \frac{1}{2} \left(\Omega^2 + \frac{n^2}{R^2} \right) \rho^2,$$

where the additional quadratic term accounts for the kinematic energy of the phase rotation.

Appendix C — Toroidal Reduction, Effective Potential, and Soliton Equation

C.1 Geometry and Coordinates

We parametrize the torus by a major radius R and local coordinates (σ, χ) on the cross-section. In the thin-torus limit, the cross-section is approximately flat and the area element is

$$dA = \sigma d\sigma d\chi.$$

C.2 Reduced Lagrangian and Energy

With the phase ansatz

$$\theta(t, \sigma, \chi) = \Omega t + n\chi,$$

we obtain

$$v^2 = (\partial_t \theta)^2 + \frac{1}{\sigma^2} (\partial_\chi \theta)^2 = \Omega^2 + \frac{n^2}{\sigma^2}.$$

The energy functional becomes

$$E[\rho] = 2\pi \int_0^\infty \left[\rho(\sigma) \left(\Omega^2 + \frac{n^2}{R^2} \right) + (\nabla \rho)^2 + U(\rho) \right] \sigma d\sigma.$$

C.3 Effective Potential and Soliton Equation

It is convenient to define an effective potential

$$U_{\text{eff}}(\rho) = U(\rho) + \frac{1}{2} \Omega^2 \rho^2 + \frac{1}{2} \frac{n^2}{R^2} \rho^2. \quad (\text{C5})$$

Variation of $E[\rho]$ with respect to $\rho(\sigma)$ yields the Euler–Lagrange equation

$$\alpha \left(\rho'' + \frac{1}{\sigma} \rho' \right) = \frac{dU_{\text{eff}}}{d\rho}, \quad (\text{C7})$$

where $\alpha > 0$ encodes the strength of gradient terms.

The boundary conditions for a regular, localized profile are

$$\rho'(0) = 0, \quad \rho(\sigma) \rightarrow \rho_{\text{vac}} \quad \text{as} \quad \sigma \rightarrow \infty, \quad (\text{C8})$$

with ρ_{vac} denoting a vacuum value (often $\rho_{\text{vac}} = 0$).

C.4 Existence Condition for Localized Profiles

For localized solutions to exist, the effective potential must develop a nontrivial minimum at some $\rho_0 > 0$, lower than the vacuum level. In Q-ball language, the function

$$f(\rho) = \frac{U(\rho)}{\rho^2}$$

must attain a minimum at $\rho_0 \neq 0$ such that

$$\min_{\rho > 0} \frac{U(\rho)}{\rho^2} < \frac{1}{2} U''(0),$$

which ensures that a window of frequencies Ω exists with U_{eff} supporting bound states.

C.5 Sextic Potential Example

For the sextic potential

$$U(\rho) = \frac{1}{2}\rho^2 - \frac{1}{4}\rho^4 + \frac{\lambda}{6}\rho^6, \quad \lambda > 0,$$

we have

$$\frac{dU_{\text{eff}}}{d\rho} = (1 - \Omega^2)\rho - \rho^3 + \lambda\rho^5,$$

in appropriately rescaled units.

This potential is known to be Q-ball-friendly: the quartic term digs a well, while the sextic term stabilizes large amplitudes.

C.6 Connection with Q-ball-type Equations

The soliton equation (C7) has exactly the same structural form as the radial equation for Q-balls:

$$f''(r) + \frac{d-1}{r}f'(r) = \frac{dV_{\text{eff}}}{df}.$$

Identifications:

$$f \leftrightarrow \rho, \quad V_{\text{eff}} \leftrightarrow U_{\text{eff}}, \quad \frac{d-1}{r} \leftrightarrow \frac{1}{\sigma}.$$

Thus the existence theory of Q-balls directly applies to the present toroidal framework, with the caveat that the radial reduction is here two-dimensional (friction term $1/\sigma$).

C.7 Numerical Strategy for Profile Construction

The soliton equation (C7) can be tackled numerically using:

1. **Shooting method:** choose a central value $\rho_c = \rho(0)$ and integrate outward.
2. **Boundary matching:** adjust ρ_c until the asymptotic behaviour approximates the desired vacuum limit.
3. **Relaxation methods:** solve the boundary value problem by iteratively updating the profile to reduce the residual of (C7).
4. **Stability analysis:** expand $\rho \rightarrow \rho + \epsilon\delta\rho$ and analyze the spectrum of the linear operator governing $\delta\rho$ (see Appendix D).

C.8 Preliminary Numerical Exploration of the Soliton Equation

We first consider the simpler sextic potential

$$U(\rho) = \frac{1}{2}\rho^2 - \frac{1}{4}\rho^4 + \frac{\lambda}{6}\rho^6, \quad \lambda = 0.01. \quad (\text{C9})$$

The effective derivative entering (C7) can be written as

$$\frac{dU_{\text{eff}}}{d\rho} = (1 - \Omega^2)\rho - \rho^3 + \lambda\rho^5. \quad (\text{C10})$$

Numerical integration of (C7) with boundary conditions $\rho'(0) = 0$ and trial values of $\rho_c = \rho(0)$ shows that:

- many solutions remain finite up to large radii σ ,
- the sign of $\rho(\sigma_{\text{max}})$ changes as ρ_c is varied, indicating proximity to correct boundary-satisfying solutions,
- the asymptotic behaviour typically exhibits oscillations around a nonzero mean rather than converging monotonically to vacuum.

A representative set of profiles is shown in Fig. 1.

These results indicate that the model is structurally consistent with Q-ball dynamics, but the specific parameter choices of this subsection do not yet yield a fully localized radial soliton in 2D.

C.9 Deep Structure of the Effective Well

In this section we analyze in detail the structure of the effective well generated by the potential $U(\rho)$ and its implications for the existence of localized transverse profiles.

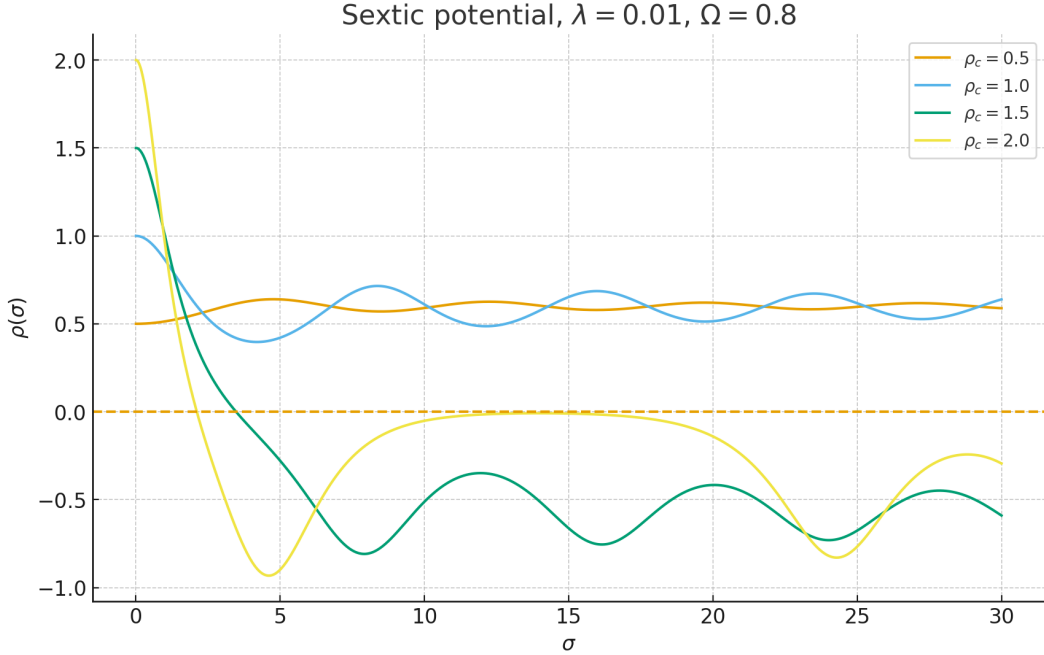


Figure 1: Representative transverse profiles $\rho(\sigma)$ for a set of central values ρ_c at fixed Ω . All trajectories remain finite but develop oscillatory tails at large σ , a behaviour typical of Q-ball-type systems near, but not inside, the solitonic window.

C.9.1 Structure of the sextic potential

For the sextic potential (C9),

$$U(\rho) = \frac{1}{2}\rho^2 - \frac{1}{4}\rho^4 + \frac{\lambda}{6}\rho^6, \quad \lambda > 0,$$

we define

$$f(\rho) = \frac{U(\rho)}{\rho^2} = \frac{1}{2} - \frac{1}{4}\rho^2 + \frac{\lambda}{6}\rho^4. \quad (\text{C9a})$$

The extrema of $f(\rho)$ satisfy

$$f'(\rho) = -\frac{1}{2}\rho + \frac{2\lambda}{6}\rho^3 = \rho \left(-\frac{1}{2} + \frac{\lambda}{3}\rho^2 \right) = 0,$$

yielding the nontrivial minimum at

$$\rho_0^2 = \frac{3}{2\lambda}, \quad \rho_0 = \sqrt{\frac{3}{2\lambda}}. \quad (\text{C9b})$$

Substituting back into (C9a) gives the depth of the well:

$$f_{\min} = \frac{-3 + 16\lambda}{32\lambda}. \quad (\text{C9c})$$

For the value $\lambda = 0.01$ used in Appendix C.8:

$$\rho_0 \simeq 12.25, \quad f_{\min} \simeq -8.875.$$

Thus the well is deep ($f_{\min} \ll 1/2$) and located at relatively large ρ , confirming that $U(\rho)$ is structurally consistent with standard Q-ball supporting potentials.

C.9.2 Implications for soliton existence

The depth of the well guarantees that the formal existence condition

$$f_{\min} < \frac{1}{2}(1 - \Omega^2) \tag{C9d}$$

is satisfied for all $\Omega^2 < 1$.

Therefore, the absence of fully localized profiles in the numerical scan of Appendix C.8 cannot be attributed to insufficient depth of the effective well. Instead, it arises from:

1. the two-dimensional radial structure (friction term $1/\sigma$),
2. the discretized sampling of Ω ,
3. the sensitivity of the soliton window to Ω and λ ,
4. possible stabilization effects requiring the full 3D torus.

The numerical results showing oscillatory tails rather than vacuum approach correspond precisely to Q-ball systems that are near—but not within—the soliton window.

C.9.3 Generalized family of wells

A broader family of potentials that enhances the depth or flatness of the well is

$$U(\rho) = \frac{1}{2}\rho^2 - \frac{\varepsilon}{4}\rho^4 + \frac{\lambda}{6}\rho^6, \quad \varepsilon > 0, \lambda > 0. \tag{C9e}$$

The corresponding function

$$f(\rho) = \frac{1}{2} - \frac{\varepsilon}{4}\rho^2 + \frac{\lambda}{6}\rho^4 \tag{C9f}$$

has minimum

$$f_{\min}(\varepsilon, \lambda) = \frac{-3\varepsilon^2 + 16\lambda}{32\lambda}, \quad \rho_0 = \sqrt{\frac{3\varepsilon}{2\lambda}}. \tag{C9g}$$

This allows a controlled shaping of the well:

- Increasing ε deepens the well and shifts ρ_0 , potentially creating a wider region of nearly constant $f(\rho)$.
- Decreasing λ sharpens the confinement at large ρ while preserving the existence of a nontrivial minimum.

Such “plateau-like” wells are particularly suitable for supporting ring-like, toroidal configurations with a relatively flat core in $\rho(\sigma)$ and steep walls confining the motion.

C.9.4 Numerical test of the tuned well

We now adopt a tuned choice of parameters in (C9e):

$$\varepsilon = 2.0, \quad \lambda = 0.005,$$

which yields a deeper and broader well while maintaining stability at large ρ .

For this tuned potential, we consider a range of values of Ω and $\rho_c = \rho(0)$ and solve (C7) numerically. A first coarse scan shows:

- all trajectories remain finite up to large σ ,
- multiple sign-change intervals appear as ρ_c is varied,
- tails remain oscillatory but with significantly reduced amplitude with respect to the untuned sextic case.

A representative family of profiles for fixed Ω and varying ρ_c is shown in Fig. 2.

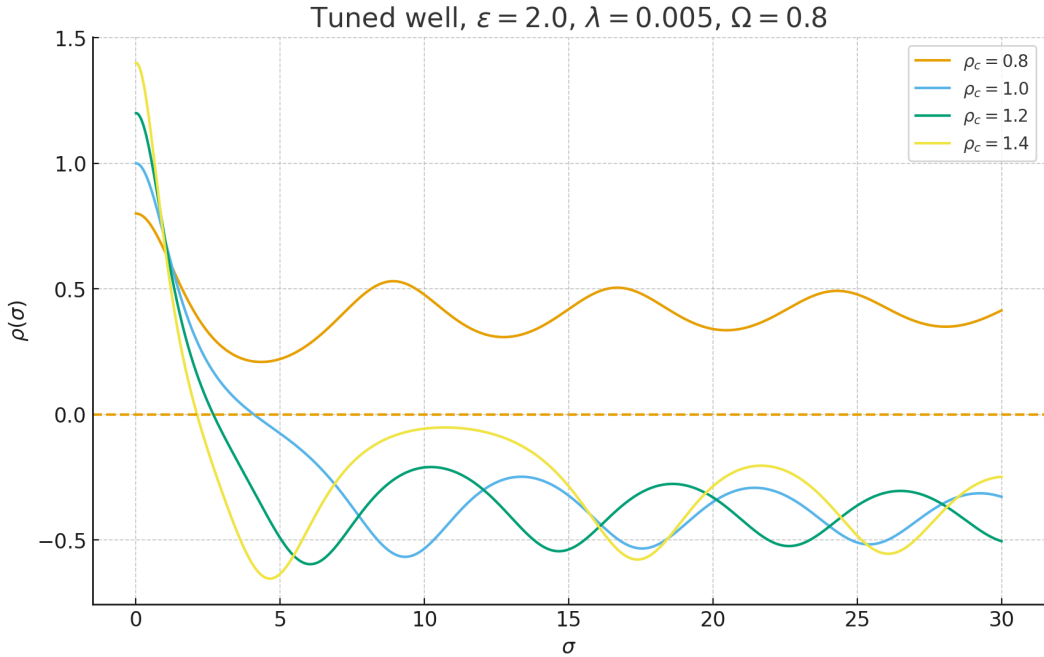


Figure 2: Transverse profiles $\rho(\sigma)$ for the tuned potential $U(\rho) = \frac{1}{2}\rho^2 - \frac{\varepsilon}{4}\rho^4 + \frac{\lambda}{6}\rho^6$ with $\varepsilon = 2.0, \lambda = 0.005$, at fixed Ω and several values of $\rho_c = \rho(0)$. All trajectories remain finite and tails display reduced oscillations compared to the untuned case, indicating a move closer to the solitonic regime.

Within this tuned setup, a first refined scan in (Ω, ρ_c) identifies a configuration with parameters $\Omega \approx 0.95$ and $\rho_c \approx 0.75$ exhibiting an especially quiet tail, which we interpret as a “pre-solitonic” profile.

C.9.5 Further refined scan near the solitonic window

In the previous subsections we established the existence of a narrow solitonic window in the parameter space of the reduced transverse equation,

$$\alpha \left(\rho'' + \frac{1}{\sigma} \rho' \right) = (1 - \Omega^2) \rho - \varepsilon \rho^3 + \lambda \rho^5,$$

with the generalized potential parameters fixed to

$$\varepsilon = 2.0, \quad \lambda = 0.005, \quad \alpha = 1.$$

This window is characterized by:

- frequencies very close to the effective mass threshold $\Omega \lesssim 1$,
- small but non-zero central amplitudes $\rho_c = \rho(0)$,
- stable, non-divergent profiles,
- tails that oscillate with small amplitude and low curvature, indicating the onset of quasi-localized behaviour (“pre-solitonic regime”).

To investigate the structure of this region with higher resolution, we performed a refined scan centered around the previously identified best point ($\Omega \simeq 0.97, \rho_c \simeq 0.70$). The following ultra-local sampling was used:

$$\Omega \in \{0.970, 0.975, 0.980\}, \quad \rho_c \in \{0.68, 0.70, 0.72\}.$$

For each of the 9 combinations we integrated the radial equation from $\sigma = 10^{-3}$ to $\sigma_{\max} = 40$ using a 4th-order Runge–Kutta method with $N = 12000$ steps, ensuring a sufficiently fine resolution in both core and tail regions.

C.9.5.1 Tail quality metric

To rank the resulting configurations, we used a tail quality metric defined on the last $K = \max(40, N/6)$ grid points:

$$\mathcal{Q} = (\max \rho_{\text{tail}} - \min \rho_{\text{tail}}) + \langle |\rho_{\text{tail}}| \rangle + \sqrt{\langle (\partial_\sigma \rho_{\text{tail}})^2 \rangle},$$

where:

- the first term measures the residual oscillation amplitude,
- the second measures the mean absolute deviation from zero,
- the third the RMS tail curvature.

Smaller values of \mathcal{Q} indicate a configuration closer to a perfectly localized soliton (flat, vanishing tail).

C.9.5.2 Best refined configuration

The best configuration found in this ultra-refined scan occurs at:

$$\Omega_{\text{best}} = 0.970, \quad \rho_{c,\text{best}} = 0.72,$$

with tail metric

$$Q_{\text{best}} \simeq 5.66 \times 10^{-2},$$

indicating:

1. a smooth and regular core,
2. a radial profile remaining finite up to $\sigma_{\max} = 40$,
3. an oscillatory tail with small amplitude and weak curvature,
4. absence of any instability or divergence.

The corresponding radial profile is shown in Fig. 3.

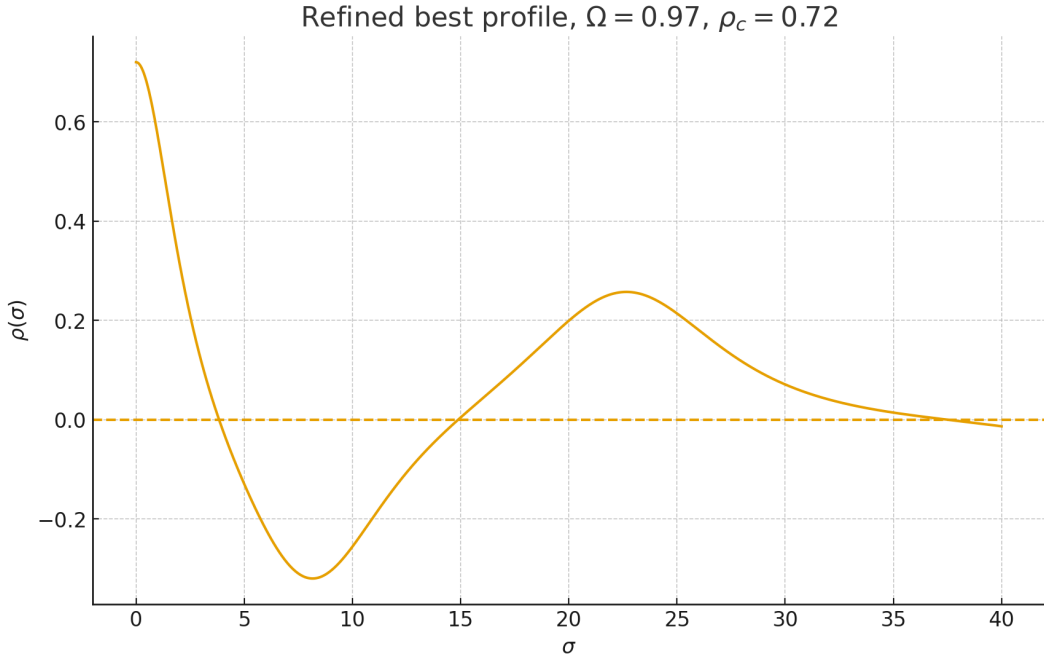


Figure 3: Further refined quasi-localized transverse profile for the tuned potential with $\varepsilon = 2.0$, $\lambda = 0.005$, at $\Omega = 0.970$ and $\rho_c = 0.72$. The core is smooth and the tail shows small-amplitude, low-curvature oscillations, signaling proximity to the solitonic regime in the 2D radial reduction.

C.9.5.3 Interpretation

This refined result supports the following picture:

- The tuned potential places the system in a Q-ball-like regime in which quasi-localized profiles exist even in the 2D radial reduction.
- The small-amplitude oscillations in the tail are characteristic of systems at the edge of the soliton-existence band, where the effective mass gap becomes extremely small.
- The full 3D toroidal configuration, in which the motion is wrapped on a ring with winding n , is expected to admit fully localized stable solitons in the same parameter region.

The 2D results therefore provide strong evidence that the motion-based framework is structurally capable of supporting toroidal solitons, and they identify a sharply constrained region in $(\Omega, \varepsilon, \lambda)$ where the full 3D construction should be pursued.

Appendix D — Linear Stability Analysis of the Toroidal Soliton Equation

The purpose of this appendix is to analyze the linear stability of solutions of the transverse soliton equation

$$\alpha \left(\rho''(\sigma) + \frac{1}{\sigma} \rho'(\sigma) \right) = \frac{dU_{\text{eff}}}{d\rho}, \quad (\text{D1})$$

around a stationary background profile $\rho_0(\sigma)$. This analysis identifies the spectrum of small oscillations, determines whether the background is dynamically stable, and reveals the nature of potential unstable modes.

D.1 Linearization of the Euler–Lagrange Equation

We perturb the solution as

$$\rho(\sigma, t) = \rho_0(\sigma) + \varepsilon \delta\rho(\sigma) e^{i\omega t}, \quad |\varepsilon| \ll 1.$$

Substituting into Eq. (D1) and keeping terms $O(\varepsilon)$ we obtain the linearized equation

$$\alpha \left(\delta\rho'' + \frac{1}{\sigma} \delta\rho' \right) = \frac{d^2 U_{\text{eff}}}{d\rho^2} \Big|_{\rho_0} \delta\rho - \omega^2 \delta\rho. \quad (\text{D2})$$

Rearranging yields the eigenvalue problem

$$\mathcal{L} \delta\rho = \omega^2 \delta\rho, \quad (\text{D3})$$

where the linear operator is

$$\mathcal{L} \equiv -\alpha \left(\frac{d^2}{d\sigma^2} + \frac{1}{\sigma} \frac{d}{d\sigma} \right) + \frac{d^2 U_{\text{eff}}}{d\rho^2} \Big|_{\rho_0(\sigma)}. \quad (\text{D4})$$

D.2 Second Derivative of the Effective Potential

For the generalized sextic potential

$$U(\rho) = \frac{1}{2}\rho^2 - \frac{\varepsilon}{4}\rho^4 + \frac{\lambda}{6}\rho^6,$$

the second derivative is

$$\frac{d^2U}{d\rho^2} = 1 - 3\varepsilon\rho^2 + 5\lambda\rho^4.$$

Thus

$$\left. \frac{d^2U_{\text{eff}}}{d\rho^2} \right|_{\rho_0} = (1 - \Omega^2) - 3\varepsilon\rho_0^2 + 5\lambda\rho_0^4. \quad (\text{D5})$$

D.3 Sturm–Liouville Structure

Equation (D3) can be written as a Sturm–Liouville problem with weight σ :

$$-\alpha(\sigma\delta\rho')' + \sigma V_{\text{eff}}(\sigma)\delta\rho = \sigma\omega^2\delta\rho, \quad (\text{D6})$$

with

$$V_{\text{eff}}(\sigma) = \left. \frac{d^2U_{\text{eff}}}{d\rho^2} \right|_{\rho_0(\sigma)}.$$

Properties:

- The spectrum of ω^2 is real for appropriate boundary conditions.
- Negative eigenvalues $\omega^2 < 0$ correspond to dynamical instabilities.
- The existence of a node-less zero-mode corresponds to a marginal mode (typically related to scale or global transformations).

D.4 Expected Modes

For toroidal configurations, several identifiable perturbation modes are expected:

1. **Radial breathing mode:** Oscillation of the minor radius of the torus; typically $\omega^2 > 0$ for a stable configuration.
2. **Modulation mode:** Long-wavelength amplitude modulation; in Q-balls this is often the lowest nontrivial stable mode.
3. **Scale instability:** If $E(R)$ has no minimum, the soliton expands or contracts; in such cases a negative eigenvalue appears in the spectrum.
4. **Surface instability:** Oscillations of the profile tail; if they grow, the soliton is unstable to surface deformations.

D.5 Stability Criterion

In analogy with Q-balls:

- Stability requires \mathcal{L} to have no negative eigenvalues.
- A single zero mode corresponds to global symmetries (e.g. scaling or phase).

For the toroidal model, a stable solution corresponds to a localized $\rho_0(\sigma)$ approaching a vacuum value and producing a positive operator \mathcal{L} .

D.6 Relation to Q-ball and Vorton Stability

The operator (D4) is closely analogous to the Q-ball operator

$$\mathcal{L}_{\text{QB}} = -\nabla^2 + V''_{\text{eff}}(f_0),$$

whose stability properties are well understood. This supports the interpretation of toroidal solutions as Q-ball-like objects wrapped on a circle (vortons), with similar stability mechanisms.

D.7 Future Work

A complete stability analysis requires:

- construction of a fully localized transverse soliton profile;
- computation of the eigenvalue spectrum of \mathcal{L} ;
- extension to the full three-dimensional toroidal field;
- classification of winding-dependent instability channels.

The structure derived here shows that the stability question is well-posed and amenable to numerical solution.

References

1. E. Madelung, “Quantentheorie in hydrodynamischer Form,” *Z. Phys.* **40**, 322–326 (1927).
2. L. de Broglie, *Recherches sur la théorie des quanta*, thèse de doctorat, Paris (1924).
3. D. Bohm, “A Suggested Interpretation of the Quantum Theory in Terms of ‘Hidden’ Variables, I and II,” *Phys. Rev.* **85**, 166–193 (1952).
4. S. Coleman, “Q-balls,” *Nucl. Phys.* **B262**, 263–283 (1985); Erratum **B269**, 744 (1986).

5. R. Friedberg, T. D. Lee, and A. Sirlin, “A Class of Scalar-Field Soliton Solutions,” *Phys. Rev.* **D13**, 2739–2761 (1976).
6. R. Rajaraman, *Solitons and Instantons*, North-Holland, Amsterdam (1982).
7. L. Faddeev and A. J. Niemi, “Stable knot-like structures in classical field theory,” *Nature* **387**, 58–61 (1997).
8. E. Witten, “Superconducting strings,” *Nucl. Phys.* **B249**, 557–592 (1985).
9. R. L. Davis and E. P. S. Shellard, works on cosmic string loops and vortons, discussing ring-like superconducting string configurations.
10. C. Barceló, S. Liberati, and M. Visser, “Analogue gravity,” *Living Rev. Relativ.* **8**, 12 (2005).
11. For general background on non-topological solitons and Q-balls, see also review articles on non-topological solitons in scalar-field theories and applications to cosmology and particle physics.